Kobe University Repository : Kernel

PDF issue: 2026-04-16

Quantification of moisture flux from the wall surface in contact with the ground in a semi-underground space based on measurements and hygrothermal analysis

Yuan, Lu
Takada, Satoru
Nagano, Yota
Fukui, Kazuma

(Citation)
Journal of Building Engineering,73:106803

(Issue Date)
2023-08-15

(Resource Type)
journal article

(Version)
Accepted Manuscript

(Rights)
© 2023 Elsevier Ltd.
This manuscript version is made available under the Creative Commons Attribution-NonCommercial-NoDerivatives 4.0 International license.

(URL)
https://hdl.handle.net/20.500.14094/0100483066

KOBE UNIVERSITY

Quantification of moisture flux from the wall surface in contact with the ground in a semi-underground space based on measurements and hygrothermal analysis

Lu Yuan, Satoru Takada, Yota Nagano, Kazuma Fukui
Kobe University, Japan

Highlights

- Quantified seasonal moisture generation from the ground in a semi-underground space.
- Quantified influence of the moisture balance of the semi-underground space.
- Moisture from ground has a greater effect on the space in winter due to heat capacity.
- Quantified moisture buffering effect of the interior wall in a semi-underground space.
- Annual measurements of underground space validated the analytical hygrothermal model.

Abstract

Relative humidity tends to be high in underground spaces. One possible cause for this is the moisture flux from the ground, whose effects have rarely been explicitly evaluated. To quantify the influence of moisture flux from the ground on indoor humidity, we performed a year-round field measurement of an unoccupied semi-underground apartment and developed a whole-building hygrothermal analysis of the target room and the surrounding ground. The larger measured annual average indoor absolute humidity than that of outdoor air indicated that the moisture transferred from the ground increased indoor humidity. Furthermore, the calculation results reproducing the measured indoor humidity confirmed the significant influence of moisture flux from the ground on indoor climate by comparing the results of a model in which the moisture flux from the ground was hypothetically masked out. The calculated indoor air moisture balance showed that the moisture flux from the envelopes in contact with the ground was more dominant than that from other envelopes or outdoor air, and that it accounted for more than 80 % of the total indoor moisture gain, except in July. The moisture flux was highest in winter (October-January) because the higher temperature of the walls in contact with the ground accelerated moisture evaporation owing to the heat capacity of the ground. This study quantitatively demonstrated the influence of the moisture flux from the ground in a real, uninhabited underground room and the mechanism of its seasonal variations. The findings will contribute to developing countermeasures against high humidity in underground spaces.

Keywords

underground room, ground, indoor hygrothermal environment, hygrothermal analysis, measurement

1. Introduction

Residential buildings and storage rooms, including those in museums and libraries, are often built underground because of the stable temperature in the ground [1-5] as well as the need for efficient use of spaces [6]. Some of these buildings and rooms are unoccupied. In addition, the relative humidity in such spaces is usually high, and can often lead to mold growth or condensation [7-10]. This relatively high humidity, characteristic of semi-underground spaces, is often attributed to a stable temperature owing

to the heat capacity of the ground, the inflow of humid air from the outdoor environment in summer, and the low temperature of the building surface exposed to the cold outdoor air in winter. Outdoor air is often considered the source of moisture that causes damage to the structural components of underground spaces. The moisture enters the rooms through air exchange by infiltration or ventilation through openings and ventilators. Another possibility is that the moisture originates in the ground, and migrates through the building envelope in contact with the ground. It is well known that moisture transfer from the ground exerts "some" effect on building envelopes in underground spaces. However, the effects of moisture transferred from the ground through building envelope have rarely been quantified for any actual building owing to the difficulties associated with measuring moisture flux from the ground. A quantitative understanding of moisture transfer from the ground is necessary to develop a method for designing underground spaces that considers moisture damage prevention and remediation measures after underground spaces are constructed.

Given the associated measurement-related limitations, numerical calculation analysis is an alternative approach to moisture transfer in underground spaces. For methods of calculating moisture transfer between the ground and building elements, EN 15026 shows the standard equations for simultaneous heat and moisture transfer for porous materials. This applies primarily to building envelopes. Several studies consider the ground without considering the moisture transfer between the ground and building envelopes from the energy consumption point of view [11-25]. Shi [26] evaluated the dehumidification effect resulting from applying a moisture buffering material to underground spaces in different climates without considering the moisture transfer between buildings and soil. In contrast, a few studies have investigated the simultaneous transfer of heat and moisture corresponding to both the ground and the building system [8,27-31]. Ogura et al. [27-29] conducted field experiments to analyze the hygrothermal condition of a fully underground space, solved the simultaneous heat and moisture transfer equations for both the ground and room, and evaluated the condensation behavior of the underground space as a function of the ventilation rate between the outdoor air and underground space. In addition, Fedorik et al. [30] investigated the effect of remediation countermeasures against condensation in basement walls based on a hygrothermal calculation, which modeled the coupling effect of heat and moisture with the ground in a simplified manner, whereas moisture transfer in the ground was not directly solved. Li et al. [8] developed a 3-D hygrothermal simulation model of an underground stone chamber, analyzed the wetting and drying behavior of the surface of the interior wall, and proposed an improved conservation method for cultural heritage.

In existing numerical studies, the high relative humidity of an underground space is always attributed to the heat capacity of the ground. As a result, most studies focused on heat transfer or temperature distribution, and the countermeasures against moisture damage owing to high humidity are usually related to insulation and the prevention of moisture transfer from outdoor air [26,30]. However, studies focusing on the influence of moisture transfer from the ground to the underground space are insufficient, and the influence of moisture flux from the ground on the underground space’s indoor climate has not yet been quantitatively compared with that of other moisture sources, such as the moisture from outdoor air and other wall structures owing to absorption/desorption processes. In addition, validation of the hygrothermal model of the underground space considering the interaction between the ground and outdoor air is very important but has not yet been fully performed for actual buildings.

This study aims to quantify the impact of the moisture flux originating from the ground and flowing through the building envelope on the hygrothermal environment of underground spaces. Because it is difficult to detect other indoor moisture sources, especially those generated by occupant behavior, the selected semi-underground room used in this study was unoccupied, eliminating the possibility that moisture was originating from human activity. The measured data were used to investigate the variations in the temperature and relative humidity in semi-underground rooms with different areas of the wall in contact with the ground in a reinforced concrete building. In addition, an analytical model of the target room, including the walls and surrounding ground, was

developed based on the simultaneous heat and moisture transfer equations. The validity of the model was evaluated by comparing calculated and measured results. Based on the model, the influence of the annual change in moisture flux from the ground to the underground space on the moisture balance of the underground space was quantified. In addition, the influence of the other walls (interior walls and a wall facing the outdoor air) was quantified. These calculations revealed the seasonal characteristics of the cause of the high humidity in underground spaces.

2. Measurement

2.1 Target and method

The target area was an unoccupied dwelling unit in an apartment building (RC structure, maisonette) in Kobe, Japan, constructed in the early 1990s. The unit is a semi-underground space that is in contact with sloping land. The north and east sides of the target dwelling unit were in contact with the ground, while the south exterior wall faced the outdoor air (Figure 1). The area proportion of the walls in contact with the ground and the walls facing the outdoor air in different rooms of the apartment are listed in Table 1. Air temperature and relative humidity were measured at 30-minute intervals in each room within the period from June 2015 to May 2019 using a temperature and humidity sensor with an integrated logger (RS-14, Especmic Corp). The measurements were based on the electrical resistance method. A thermistor was used for the temperature measurements, whereas a polymer membrane was used for the humidity measurements. The accuracy of temperature and relative humidity measurements is 0.5 °C and 5 %, respectively. The locations of the sensors in each measured room are marked in Figure 1 with blue dots. No one lived in the apartment, and none of the rooms in this dwelling unit were air-conditioned. The composition of the walls of a representative room is shown in Figure 2. Specifically, the vertical and horizontal sections of the envelopes of the “east room” on the lower floor are shown.

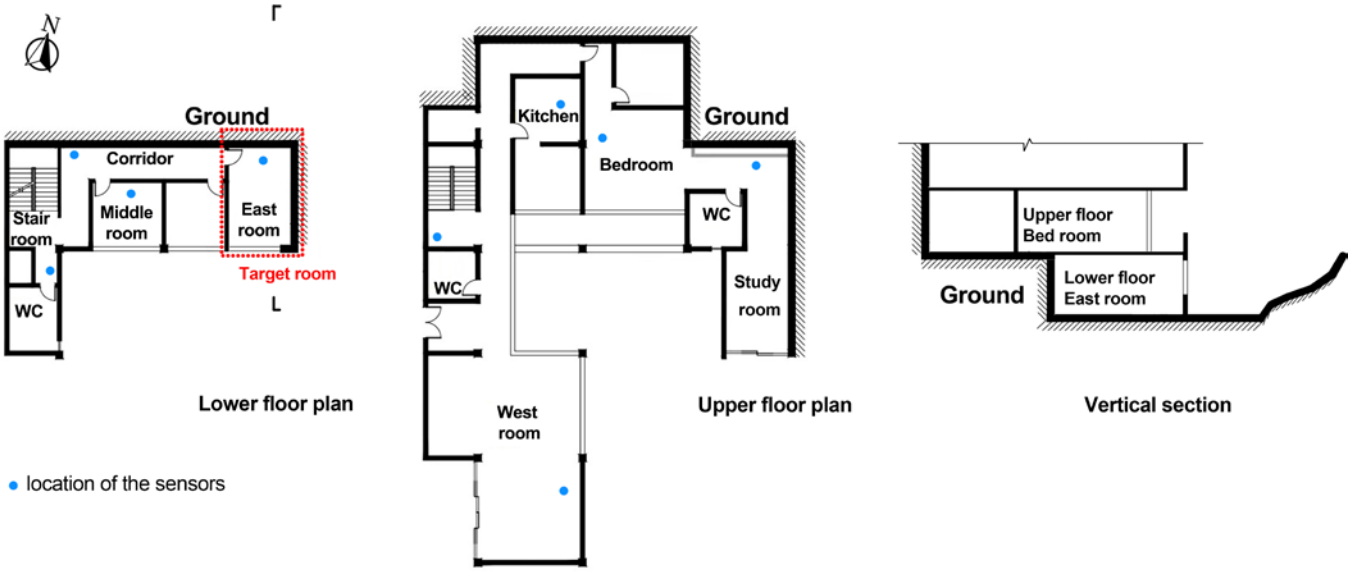

Figure 1. Floor plan and section of the target dwelling unit.

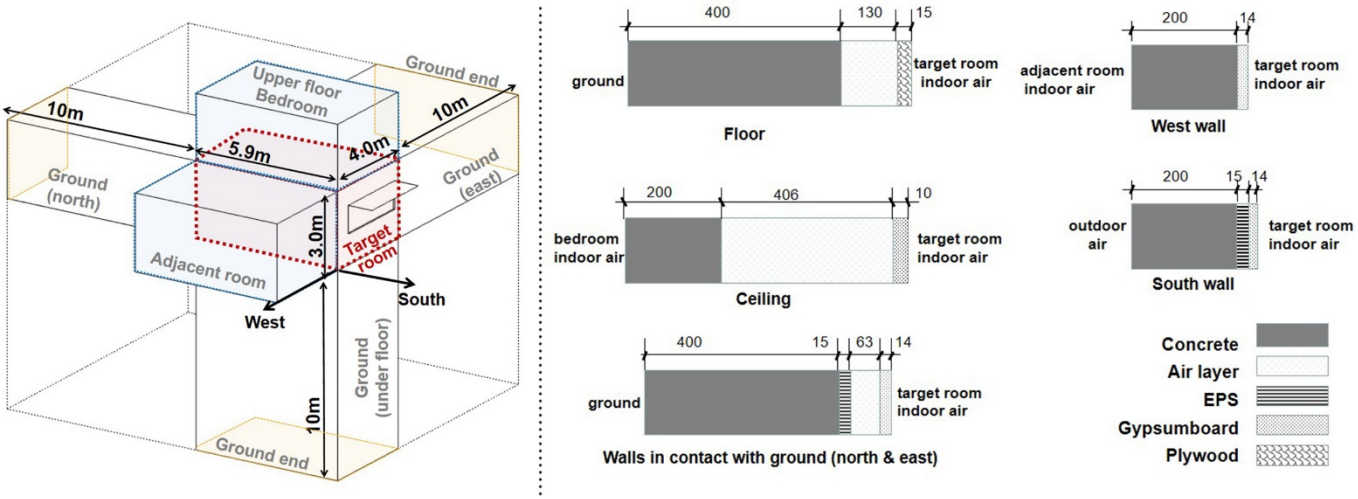

Figure 2. Composition of the building envelopes of the “east room” on the lower floor.

2.2 Results of measurement and observation

Window condensation was observed in the “study room”, “bedroom” on the upper floor, and the “east room” on the lower floor that were in contact with the ground, and condensation stains were observed on the interior surfaces of the envelopes in contact with the ground and on the interior surface of the envelopes facing the outdoor air in winter.

Figure 3(a) shows the changes in temperature in the “west room” on the upper floor, and the “east room” on the lower floor as well as the outdoor air temperature. In addition, the temperature in the “west room” was comparatively higher throughout the year owing to the higher solar radiation. Furthermore, the “east room” that had almost no solar gains, was in contact with the ground, whereas the “west room” was not (Table 1). This was also the reason for the lower annual temperature variations in the “east room”.

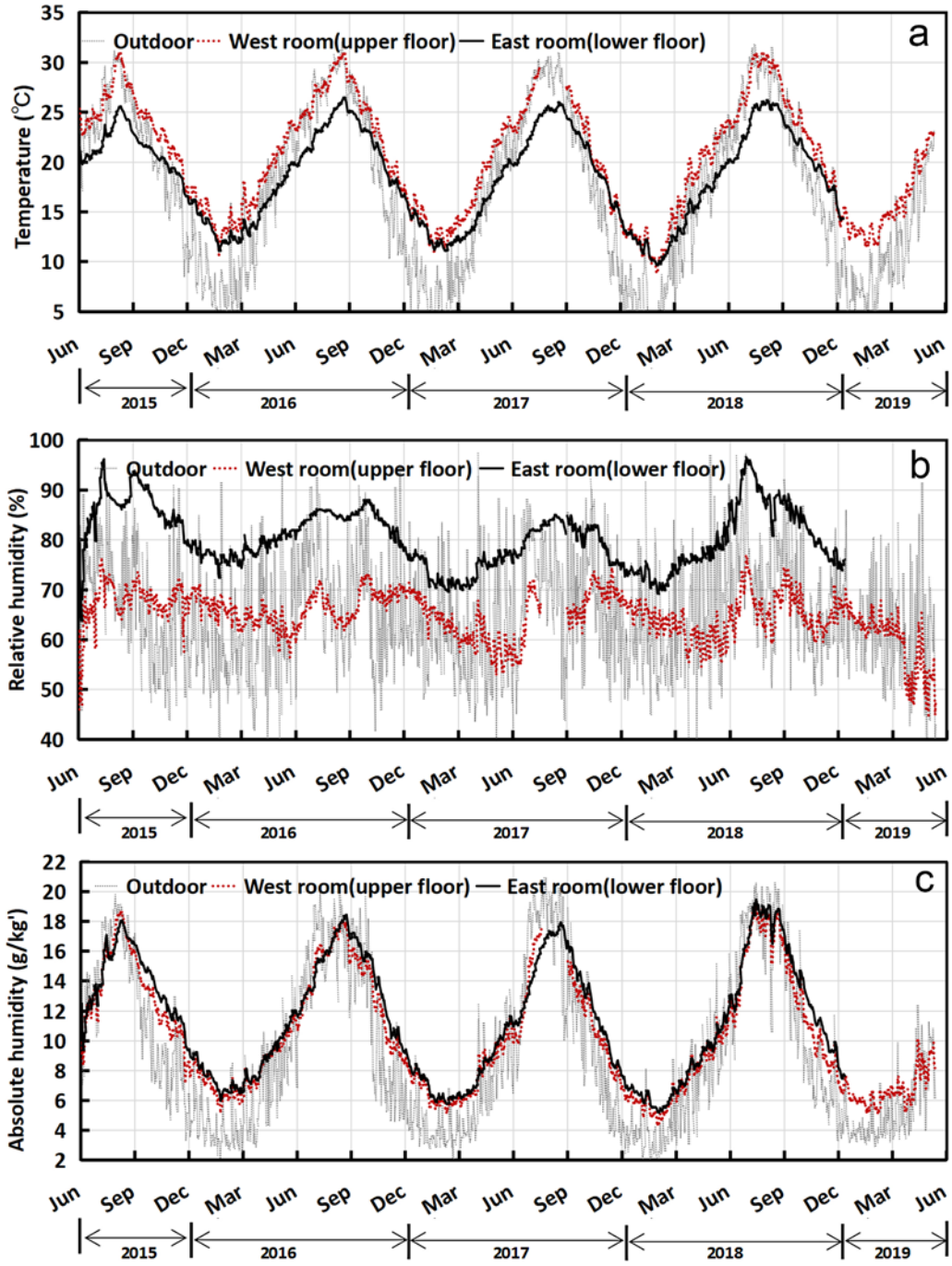

Figure 3. Measured indoor (a) temperature, (b) relative humidity, and (c) absolute humidity (daily average from June 2015 to May 2019) (West room is not in contact with the ground, while the "east room" is in contact with the ground.) (The area proportion of the envelopes in contact with the ground and those facing the outdoor air in each room are shown in Table 1).

Table 1. Area proportion of envelopes in contact with the ground and facing the outdoor air, and interior envelopes in different rooms.

	Area proportion of the envelopes in contact with ground to total envelopes of the room (m^2/m^2)	Area proportion of the envelopes facing outdoor air to total envelopes of the room (m^2/m^2)	Area proportion of the interior envelopes to total envelopes of the room (m^2/m^2)
Target room: East room (lower floor)	0.5	0.11	0.39
West room (upper floor)	0	0.38	0.62
All rooms on lower floor	0.35	0.17	0.48
All rooms on upper floor	0.22	0.21	0.57

The annual average temperatures of all rooms were higher than the annual average temperature of the outdoor air (Figure 4(a)), which can be attributed to solar radiation. Except for the "west room," solar radiation was poorly insolated. Therefore, the annual average temperature in the "west room" was higher than all other rooms closer to the ground. The annual average relative humidity in the "west room" was 66 %, whereas it varied between 75 % and 85 % in the other rooms. The "west room" had lower relative humidity over the years owing to the higher temperature compared with the "east room" which was in contact with the ground (Figure 3(b)). The absolute humidity of the interiors of the "west room" and "east room" did not differ significantly because all the rooms were connected with open doors (Figures 3(c)). Except for the "west room," all other rooms in the target dwelling unit were in contact with the ground and were at risk of condensation and mold growth.

As shown in Figure 4(b), the annual average absolute humidity in each room was higher than that of the outdoor air. Therefore, some moisture gain existed in the rooms. However, the dwelling unit in question was unoccupied, which means that there was no possibility of indoor moisture generation owing to occupant activities or any other source. This indicates that the moisture originated from the ground. In other words, the annual integrated moisture flux from the ground has a positive value. This was also supported by the fact that rooms with a greater ratio of envelopes in contact with the ground to room volume had a higher absolute humidity.

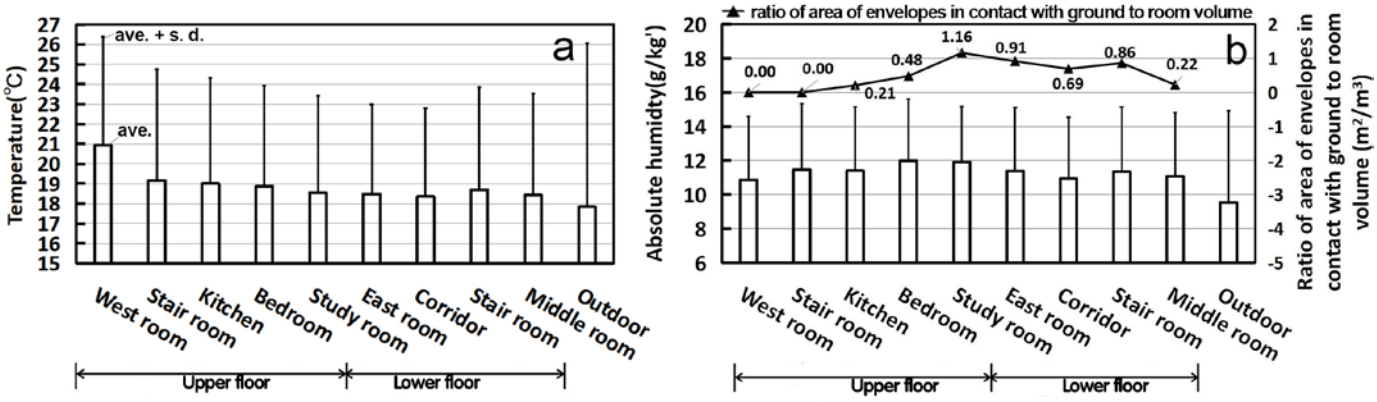

Figure 4. Measured indoor (a) temperature, and (b) absolute humidity, along with the ratio of area of envelopes in contact with the ground to the room volume (annual average and standard deviation for 2016).

3. Analysis of the hygrothermal behavior of a room connected to the ground

To quantify the hygrothermal behavior of a typical room in a semi-underground space, an analytical model based on equations for simultaneous heat and moisture transfer was adapted to the ground and building envelopes. The model was combined with the equations for the heat and moisture balance of the indoor air under the influence of the outdoor climate. The "east room" on the lower floor of the building was selected as a typical space to target for the analysis. The north and east walls of this room and its floor are in contact with the ground; the west wall and ceiling are in contact with the adjacent rooms; and the south wall is in contact with the outdoor air (Figures 1 and 2).

3.1 Calculation method

3.1.1 Fundamental equations

The analysis was performed using the WUFI Plus software [32,33]. The indoor air in the target room was treated as one node surrounded by four walls, a floor, and a ceiling. For the indoor air, the corresponding equations for heat and moisture transfer balance are as shown in Equations (1) and (2).

$$c_a \cdot \rho_a \cdot V \cdot d\theta_i / dt = \Sigma Q_{s,j} + Q_{in} + Q_{vent} \quad (1)$$

$$\rho_a \cdot V \cdot dX_i / dt = \Sigma Q'_{s,j} + Q'_{in} + Q'_{vent} \quad (2)$$

where θ_i represents the temperature of the room air [°C], c_a represents the specific heat of the room air [J/(kg·K)], ρ_a represents the density of the room air [kg/m^3], V represents the volume of the room air [m^3], t represents time [s], $Q_{s,j}$ represents the heat flow from the surface of the envelope component j to the room air [W], Q_{in} represents the heat generated in the room, including the solar radiation effect [W], and Q_{vent} represents the heat flow into the room via ventilation [W], X_i represents the absolute humidity of the room air [kg/kg']*, $Q'_{s,j}$ represents the moisture flow from the surface of the envelope component j to the room air [kg/s], Q'_{in} represents the moisture generated in the room [kg/s], and Q'_{vent} represents the moisture flow into the room owing to the ventilation [kg/s].

*kg': the mass of dry air

For the wall systems and ground, one-dimensional simultaneous heat and moisture transfer equations were assumed for each material (Equations (3) - (5)).

$$(c \cdot \rho + \partial H_w / \partial \theta) \cdot \partial \theta / \partial t = \partial / \partial x \cdot (\lambda \cdot \partial \theta / \partial x) + L \cdot \partial / \partial x \cdot (\delta_p \cdot \partial (\varphi \cdot P_{sat}) / \partial x) \quad (3)$$

$$\partial w / \partial t = \partial / \partial x \cdot (D_{ww} \cdot \partial w / \partial x) + \partial / \partial x \cdot (\delta_p \cdot \partial (\varphi \cdot P_{sat}) / \partial x) \quad (4)$$

$$w = f(\varphi) \quad (5)$$

where c represents the specific heat of the building material [J/(kg·K)], ρ represents the density of the building material [kg/m³], H_w represents the enthalpy of the building material moisture [J/m^3], λ represents the heat conductivity of the building material [J/(m·s·K)], λ' represents the moisture conductivity [kg/(m·s·Pa)], L represents the latent heat of water [J/kg], P_{sat} represents the water vapor saturation pressure [Pa], δ_p represents the vapor permeability of the porous material [kg/(m·s·Pa)], φ represents the relative humidity [-], w represents the moisture content [kg/m^3], D_{ww} represents the liquid moisture diffusivity [kg/(m^2·s)], and f represents the equilibrium moisture content [kg/m^3].

3.1.2 Calculation conditions

Table 2 summarizes the detailed internal structures of the walls, floors, and ceilings. The boundary conditions of the model are listed in Table 3. The boundary condition of the ground was set at a distance of 10 m from the outside surface of the wall. For the ground end, the temperature was considered constant at 17.3 °C, representing the annual average outdoor temperature. The humidity boundary condition was selected based on the previous research [8,20,27-30,35]. Owing to the measurement results, the

humidity in the ground at a depth of 3 m below the ground level was relatively stable over a year, and the humidity values measured at a depth of 2 m were similar to those at a depth of 3 m [27]. Because the target room was located at a depth of approximately 5 m below ground level (Figure 1), the water content of the soil surrounding the room was assumed to be stable and homogeneous in the region far enough from the room. Thus, the vertical distribution of relative humidity was neglected, and the boundary condition of the relative humidity was set at the point 10 m apart from the wall, as shown in Figure 2, with a constant value. The relative humidity boundary was constant at 99.93 %, corresponding to a 220 kg/m^3 moisture content based on the equilibrium relationship of the ground. For the surfaces of the walls facing the air, the heat and moisture fluxes were given by the difference between the surface and bulk air temperatures/vapor pressures multiplied by the transfer coefficients (Table 4). In addition, the boundaries between the materials were treated as contact conditions.

Table 2. Structure of the envelopes of the "east room" on the lower floor.

Envelope	**Constituent material**	**Thickness [m]**	**Area [m^2]**
East wall (contact with the ground)	Gypsum board Air layer EPS Concrete	0.014 0.063 0.015 0.4	12.5
North wall (contact with the ground)	Gypsum board Air layer EPS Concrete	0.014 0.063 0.015 0.4	8.18
West wall (contact with the adjacent room)	Gypsum board Concrete	0.014 0.2	12.5
South wall (facing the outdoor air)	Gypsum board EPS Concrete	0.014 0.015 0.2	4.79
South window (facing the outdoor air)	Glass	0.003	3.39
Floor (contact with the ground)	Plywood board Air layer Concrete	0.015 0.13 0.4	17.3
Ceiling (contact with the adjacent room)	Gypsum board Air layer Concrete	0.01 0.406 0.2	17.3

Table 3. Boundary conditions used in the calculations.

	Heat	Moisture
End of the ground (10 m from the surface or contact point to envelope)	Constant at 17.3 °C	Constant at 99.93 % RH
Air of adjacent room	Same temperature as that of the target room	Same absolute humidity as that of the target room
Surface facing the outdoor air	$q=\alpha(\theta_{outdoor\ air}-\theta_{surface})$	$q'=\beta(P_{outdoor\ air}-P_{surface})$

θ, temperature [°C]; RH, relative humidity [%]; P, vapor pressure [Pa]; q, heat flux [W/m^2]; q', moisture flux [kg/(m^2·s)]; α, combined heat transfer coefficient [W/(m^2·K)]; β, water vapor transfer coefficient [kg/(m^2·s·Pa)]

Table 4. Heat/moisture transfer coefficients corresponding to the surface of envelope components.

	Convective heat transfer coefficient [W/(m^2·K)]	Radiant heat transfer coefficient [W/(m^2·K)]	Water vapor transfer coefficient [kg/(m^2·s·Pa)]
Indoor side	4.65	4.65	3.26×10^{-8}*
Outdoor side	18.5	4.65	1.30×10^{-7}*

*In WUFI, the water vapor transfer coefficient β was derived from the convective heat transport coefficient α_c through analogous relations: $\beta = 7\times10^{-9}\ \alpha_c$.

The calculation period was an entire year, from January 1, 2016, to January 1, 2017. Under the initial conditions (room air temperature and relative humidity at 17 °C and 80 %, respectively, and ground and building envelope temperatures and relative humidity at 17 °C and 99.93 %, respectively), a warm-up calculation was conducted until the solutions of temperature and moisture reached a periodic steady state for the annual outdoor conditions corresponding to 2016. The process was repeated 20 times (calculated for 20 years).

Based on the measured results, the indoor air temperature and absolute humidity of the target room and the adjacent rooms did not differ significantly. Thus, in the calculation model, the rooms adjacent to the target room were regarded as having the same indoor temperature and humidity as the target room. Therefore, the ventilation between the rooms was neglected. Further, ventilation with outdoor air in the target room was treated as a constant at 0.15 ACH (equivalent to 6.3 m^3/h). In this study, the dwelling unit was uninhabited without any mechanical ventilation, and the HVAC system was off during the investigation period. The target room's window was closed. Thus, the air exchange between indoors and outdoors would almost be limited to air infiltration. The air infiltration rate value would be related to building type, floor area, number of floors, construction year, orientation of the wall, and structure material [36]. Shi et al. measured the air infiltration rates in 34 inhabited dwelling units without mechanical ventilation. They found that the air infiltration rates were influenced more significantly by the floor area than by the orientation or construction year [36]. In the target room, the stack effect or wind pressure would not significantly influence the air infiltration rate because there was no indoor heating or cooling and the window was facing a yard surrounded by other buildings. In addition, for concrete residential buildings, the air infiltration rates of 8 cases whose floor area was close to our target dwelling unit varied from 0.1 h^{-1} to 0.29 h^{-1} [36], and thus, the median value (0.15 h^{-1}) was used in our calculation. For the outdoor temperature and relative humidity, data obtained from the local Meteorological Agency were used. Diffusion and direct solar radiation effects on the wall and window facing the outdoor air were included, and considered the shading effect of the eaves

above the window. The cloud index was determined using data from the Meteorological Agency corresponding to hours of sunlight per hour. As an approximate treatment, the solar gain through the window was distributed on the inner surface of the envelopes proportional to the area.

The material properties used in the calculation, which were sourced from databases, are listed in Table 5 [32,34]. Table 4 lists the heat and water vapor transport coefficients used in the analysis.

Table 5. Material properties used in the calculations.

	Gypsum [32]	**Plywood [32]**	**EPS [32]**	**Concrete [34]**	**Ground [32]**
Density [kg/m^3]	700	454	25	2200	1361
Specific heat [J/(kg·K)]	870	1400	1225.8	800	850
Thermal conductivity [W/(m·K)]	0.22*	0.12*	0.028*	1.62*	0.318*
Porosity [m^3/m^3]	0.7	0.56	0.98	0.15	0.504
Water vapor diffusion resistance factor [-]	6.8	203	20.4	200	50
Liquid moisture diffusivity [m^2/s]	Function of moisture content	Function of moisture content	0	Function of moisture content	Function of moisture content
Equilibrium moisture content [kg/m^3]	Function of relative humidity	Function of relative humidity	Function of relative humidity	Function of relative humidity	Function of relative humidity

*Value corresponding to the dry material. In the calculations, the thermal conductivities were given as a function of the moisture content.

3.2 Results of the hygrothermal analysis

The calculation model was validated by comparing the measured hourly indoor temperature and absolute humidity with the calculated results. The calculated air temperature and absolute humidity values agreed well with the hourly measured data, as shown in Figure 5. The coefficients of determination were 0.99 for both temperature and absolute humidity (Figure 6), indicating that the calculation model was reasonable.

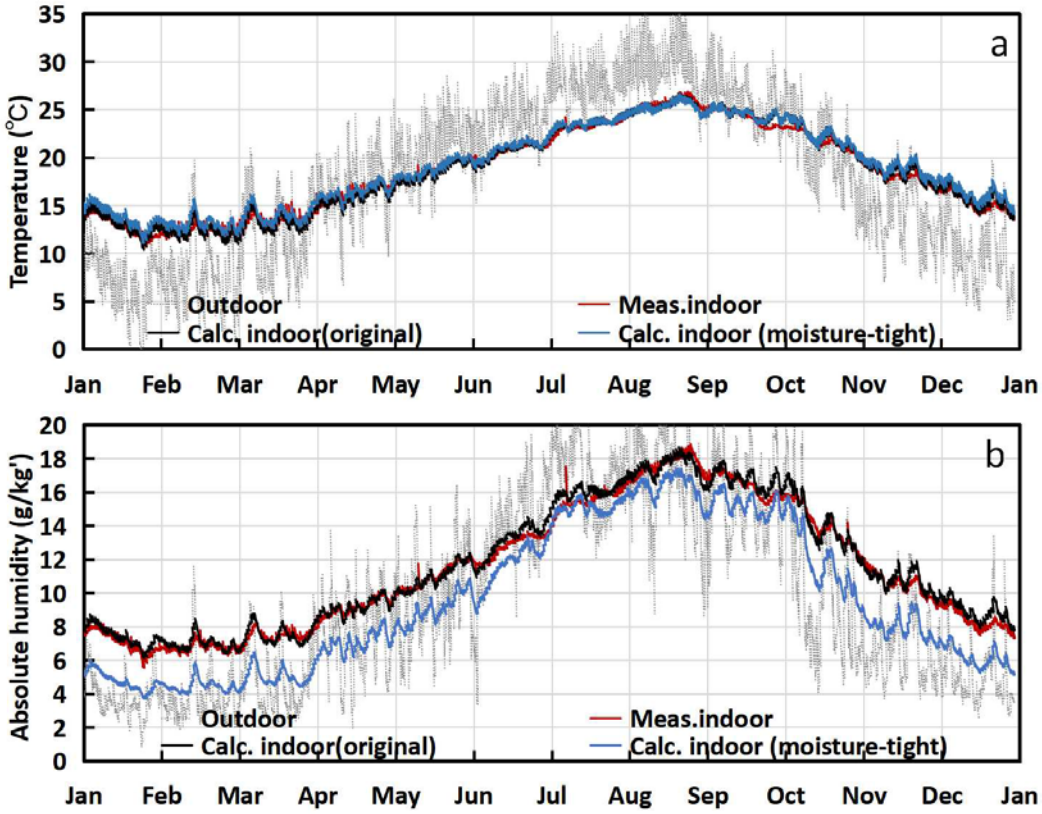

Figure 5. Measured and calculated (a) indoor temperature and (b) indoor absolute humidity. (For calculation, both the original case and the moisture-tight case, where the moisture transfer from the ground was hypothetically masked out, are shown). (hourly data for 2016).

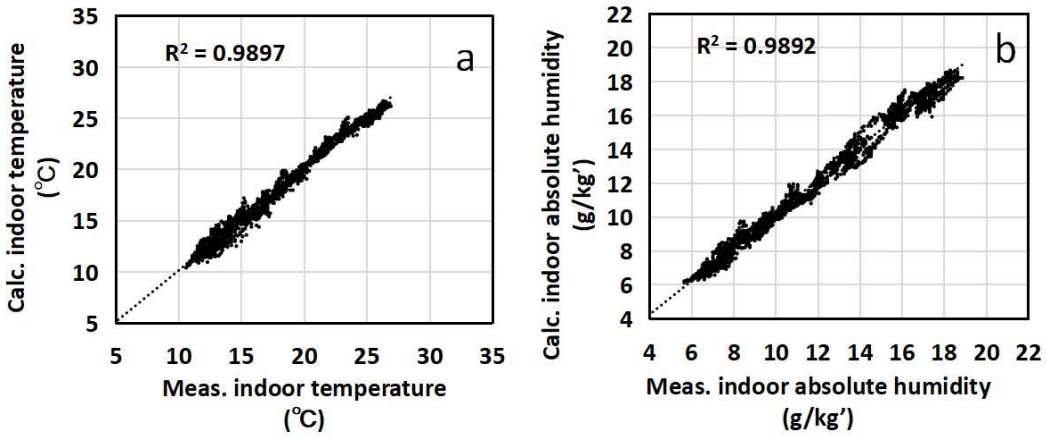

Figure 6. Correlations between measured and calculated results: (a) indoor temperature and (b) indoor absolute humidity (hourly data for 2016).

3.2.1 Heat and moisture balance of indoor air

Figure 7(a) shows the monthly average heat flux on the inner surface of the room. The net heat gain of the room air is not shown because it represents less than 0.1 % of the total heat flux transferred to the indoor air. Positive values mean heat transfer to the indoor air from the solid surfaces of the envelope. Heat transferred from the indoor air to the solid surface in winter for the

envelope facing the outdoor air (i.e., window and south wall). For the envelope in contact with the ground (i.e., the floor, east wall, and north wall), heat flowed from the surface to the indoor air in winter (i.e., from November to March). In summer, the opposite scenarios were observed, which could be attributed to the heat capacity of the ground. In addition, heat absorption by the ground in summer lowered the room air temperature, resulting in high relative humidity. The heat exchange with the outdoor air through the ventilation was lower than the heat transferred from the wall facing the outdoor air and the window.

Figure 7(b) shows the monthly average moisture flux on the interior surface of the target room. The positive values indicate that moisture was released from the solid interior surfaces of the envelopes to the room air. Specifically, for the envelope in contact with the ground (i.e., the floor, east wall, and north wall), moisture was released to the indoor air almost throughout the year, and the amount released was greater in the winter season (at especially high levels from October to March) than in summer, indicating that the walls in contact with the ground were sources of moisture to the room air. The maximum daily average value in winter was 19 g/(m^2 day) (Figure omitted). Except in June and July, ventilation was the predominant pathway for moisture leakage from the interior space, and in June and July, the interior envelopes in contact with adjacent rooms (ceiling and west wall) absorbed moisture. The interior walls have desorbed moisture, except in the summer, and act as a moisture capacity for indoor air throughout the year, accounting for no more than 20 % of the moisture balance of the room. The areas of the wall in contact with the ground, interior wall, and wall facing the outdoor air are 38m^2, 30m^2, and 5m^2, respectively (Table 2). The moisture flux from envelopes in contact with the ground was much greater than that from envelopes that were not in contact with the ground, especially in winter, despite the area of the envelopes in contact with the ground not being significantly different from that not in contact with the ground. Overall, moisture from the ground contributed most to the high indoor humidity.

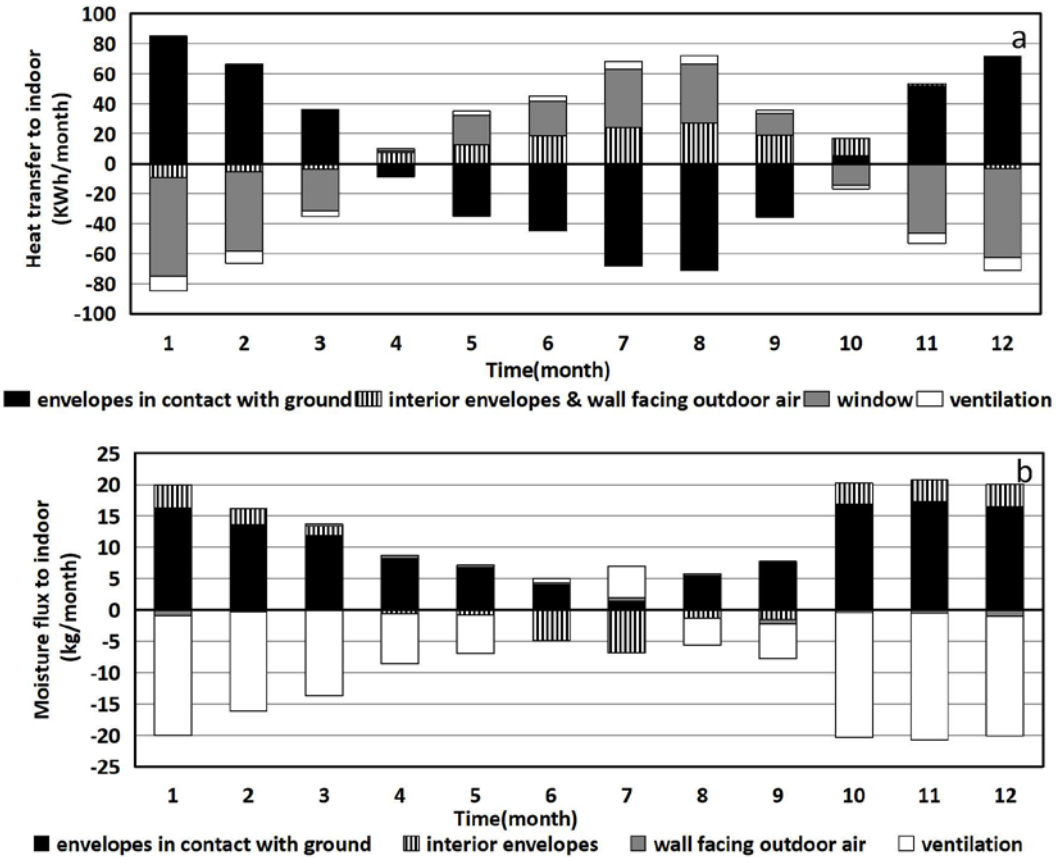

Figure 7. Calculated monthly average (a) heat balance of indoor air and (b) moisture balance of indoor air (2016).

3.2.2 Moisture fluxes from the envelopes

As shown in Figure 8, the monthly moisture flux from the floor, the wall in contact with the ground, the wall facing outdoor air, and the interior wall in different seasons were compared.

The influence of the moisture from the ground on indoor high humidity was confirmed by the fact that the moisture flux from the wall in contact with the ground was considerably larger than that from the interior wall over a year. Moreover, the comparison of the moisture flux from the floor and that from the wall in contact with the ground reveals the difference in the influence of the heat capacity of the ground on the moisture flux from the ground. The influence of the heat capacity of the ground would be more significant on the floor than on the wall in contact with the ground because the floor was not insulated. Therefore, compared with the wall in contact with the ground, the moisture flux on the floor was larger in winter and smaller in summer. For the south wall facing outdoor air, its large annual temperature fluctuation significantly impacted the moisture flux on its surface. In winter, its low temperature contributed to a smaller vapor partial pressure and made it absorb moisture from the indoor air, which could result in a risk of excessively high humidity on the indoor surface.

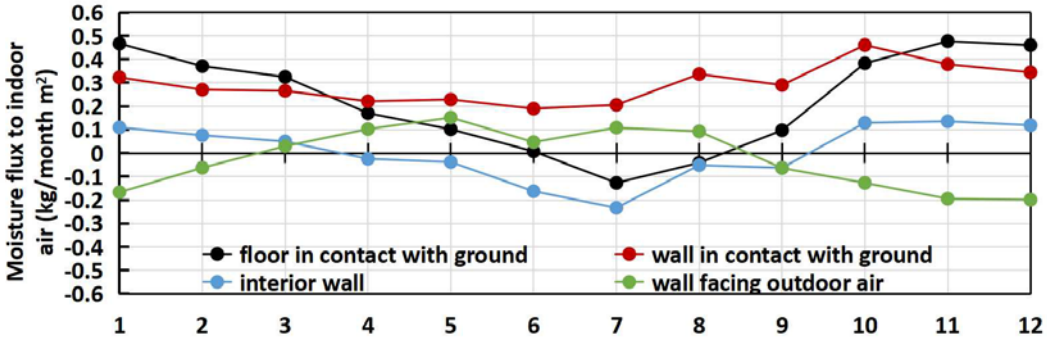

Figure 8. Calculated monthly moisture flux from the floor in contact with the ground, the wall in contact with the ground, the wall facing outdoor air, and the interior wall in the target room (2016).

3.2.3 Temperature and humidity distribution in the envelopes

As shown in Figures 7 and 8, the wall in contact with the ground released more moisture to the indoor air for most of the year compared to the interior wall and the wall facing the outdoor air. In addition, the moisture flux from the wall in contact with the ground was greater in winter than in summer. Figure 9 shows the annual changes in the distribution of temperature, relative humidity, and absolute humidity in the walls and ground.

Because the relative humidity of the ground at a depth of 10 m was set at a constant value of nearly 100 %, owing to the moisture transferred from the ground, the relative humidity of the concrete wall in contact with the ground was higher than the other walls not contacting with the ground through a year. The high liquid moisture diffusivity and moisture capacity of concrete at high humidity resulted in a small distribution and a small annual variation in relative humidity in the concrete layer. When the indoor humidity changed significantly owing to the influence of outdoor air, the relative humidity of the concrete layer fluctuated only slightly on the interior side (92–94 %). In addition, the temperature of the concrete layer in contact with the ground was higher than that of the other walls in winter owing to the heat capacity of the ground. Therefore, the absolute humidity of the wall in contact with the ground was higher in winter because of the constant high relative humidity close to saturation through a year. This resulted in a greater absolute humidity gradient in the walls near the indoor air (interior side layers of the concrete layer) and caused a greater flow of moisture from the wall side to the indoor air in winter (See the distribution of the absolute humidity in the wall layer between the indoor air and the concrete layer（gypsum, air layer, EPS）, for “November” and “January”, in Figure 9 “wall in contact with ground”).

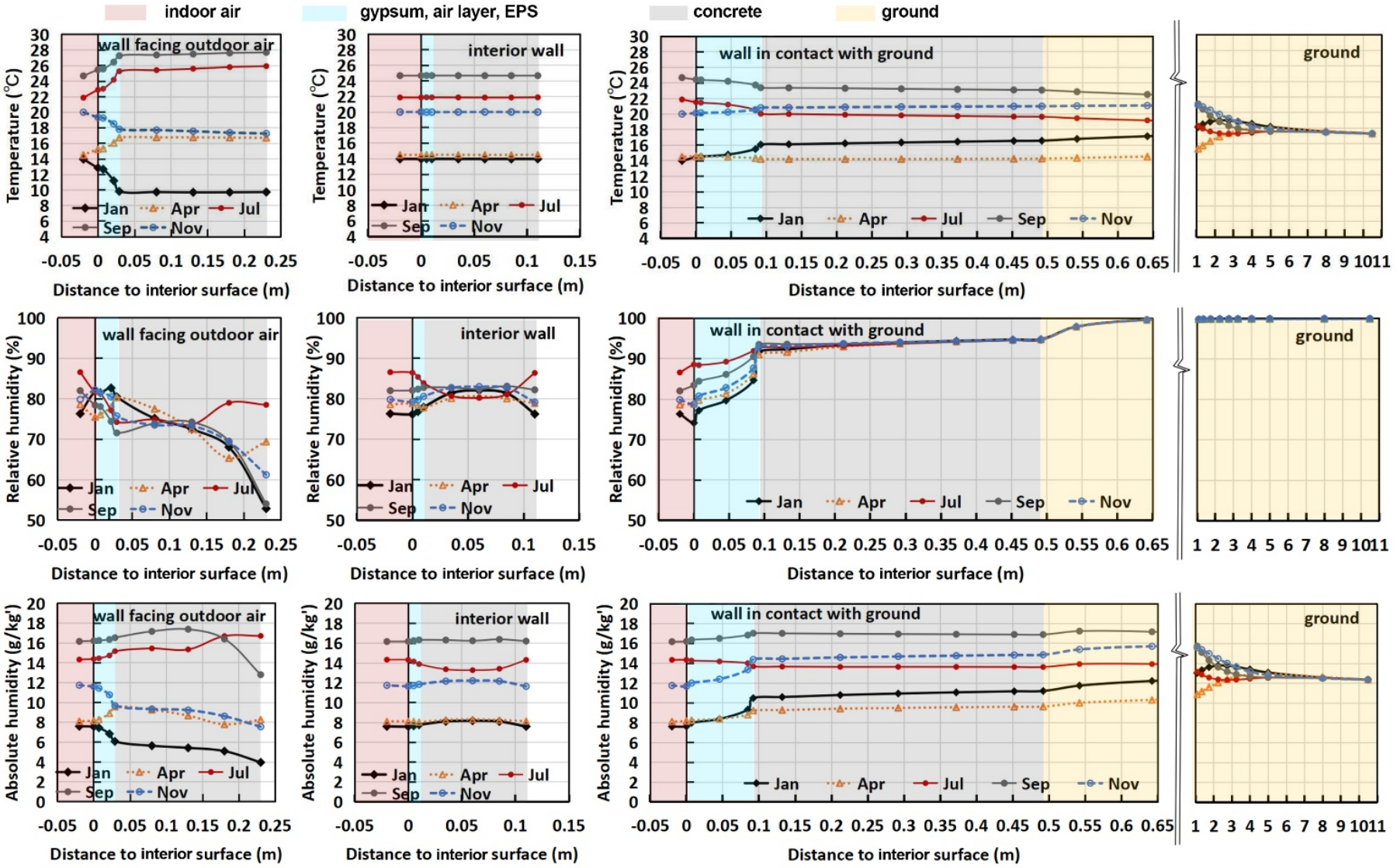

Figure 9. Annual change in temperature, relative humidity, and absolute humidity distribution in the wall facing the outdoor air, interior wall, and wall in contact with the ground (daily average value on the 1st day of the month for 2016) (The ground region from 0.65 to 1 m in horizontal axis is not described.)

3.2.4 Condensation risk in the target room

Based on the calculated results, the condensation risk of the window in each month was evaluated by the number of hours that the interior surface temperature was lower than the dew point of the indoor air. As shown in Figure 10(a), condensation occurred on the window for more than 400 h per month in winter. Figure 10(b) shows the monthly maximum interior surface relative humidity for the different walls. The relative humidity of the walls in contact with the ground was high throughout the year. This shows that despite the absence of moisture sources owing to human activities in that unoccupied target room, the noticeable moisture flux from the ground contributed to the significantly high humidity of the envelope facing the outdoor air.

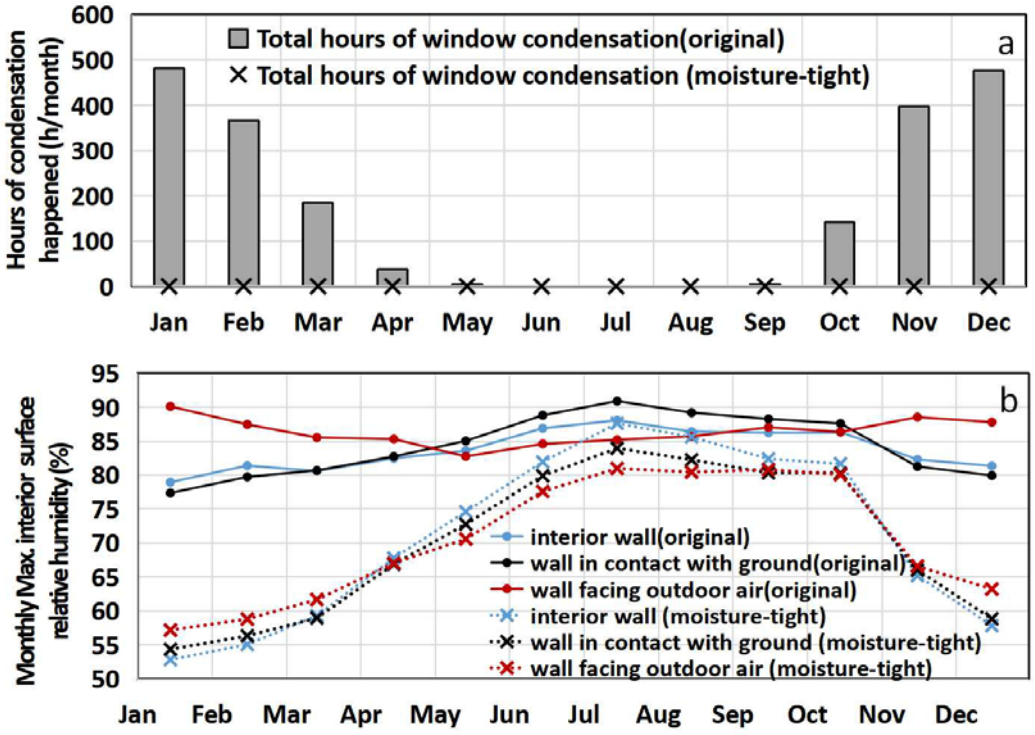

Figure 10. (a) Calculated number of hours when window condensation occurred in each month; (b) Calculated monthly maximum inner surface relative humidity of walls (Both the original case and the moisture-tight case, where the moisture transfer from the ground was hypothetically masked out, are shown) (2016).

3.3 Verification of the influence of moisture originating from the ground

To confirm the influence of moisture transfer from the ground on the humidity in our target room, another calculation was performed that included a hypothetical impermeable membrane between the ground and concrete layer of the wall. The conditions that hypothetically masked the influence of moisture transfer from the ground were analyzed.

The calculated indoor air temperature in the moisture-tight case was almost the same in summer as that obtained in the original case without masking out the moisture transfer from the ground (Figure 5), despite the temperature being slightly higher in winter owing to the lower moisture evaporation rate at the wall surfaces in contact with the ground. However, the calculated absolute humidity values, excluding moisture transfer from the ground, were significantly lower than the measured values obtained throughout the year. Moreover, it was impossible to reproduce the measured humidity trend without accounting for the moisture flow from the ground (Figure 5). The annual average of absolute humidity in our target room was similar to that of the outdoor air in the moisture-tight case (Figure 11). This shows that moisture transfer from the ground has a significant influence on indoor humidity. Figure 10(a) shows that no condensation occurs in the moisture-tight case, and Figure 10(b) shows that the relative humidity at the wall surfaces is much lower than in the original case.

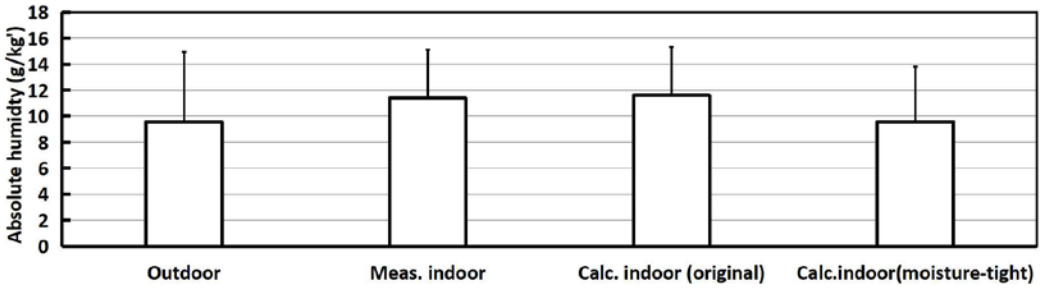

Figure 11. Calculated and measured indoor absolute humidity (annual average and standard deviation for 2016) (For calculation, both the original case and the moisture-tight case, where the moisture transfer from the ground was hypothetically masked out, are shown) (Measured outdoor absolute humidity is shown for reference).

4. Discussion

4.1 Influences of the parameters used in the calculation

4.1.1 Ground moisture boundary condition

In this study, the relative humidity at the end of the ground was treated as constant throughout the year in the calculation model. The baseline of this value might generally depend on the water table's height and ground surface conditions. In addition, this value was also influenced by precipitation and evaporation at the surface. In most cases, the ground relative humidity was assumed to be close to saturation [27], and most existing numerical analyzes assumed that the soil relative humidity was constant and above 99.9 % [8,20,28,29,30,35]. In this study, the concrete wall was assumed to be connected to the ground, and the humidity boundary conditions above 99.9 % (i.e., 99.91 %, 99.93 %, 99.95 %, 99.97 %, and 99.99 %) were tested in the calculation (Figure 12). The effect of the boundary humidity on the indoor air temperature was insignificant. Regarding the indoor absolute humidity, the differences between the cases with a boundary relative humidity of higher than 99.93 % were relatively insignificant. Only when the relative humidity was 99.91 % the calculated indoor absolute humidity did not agree with that obtained by measurement. The boundary humidity setting was sensitive owing to the sharp change in the equilibrium moisture content relationship, as shown in Figure 12 (b). Furthermore, the liquid moisture diffusivity in the range near saturation, and its influence was greater in winter than in summer. In the original case, the boundary relative humidity was set at 99.93 %, which was determined to be a reasonable assumption.

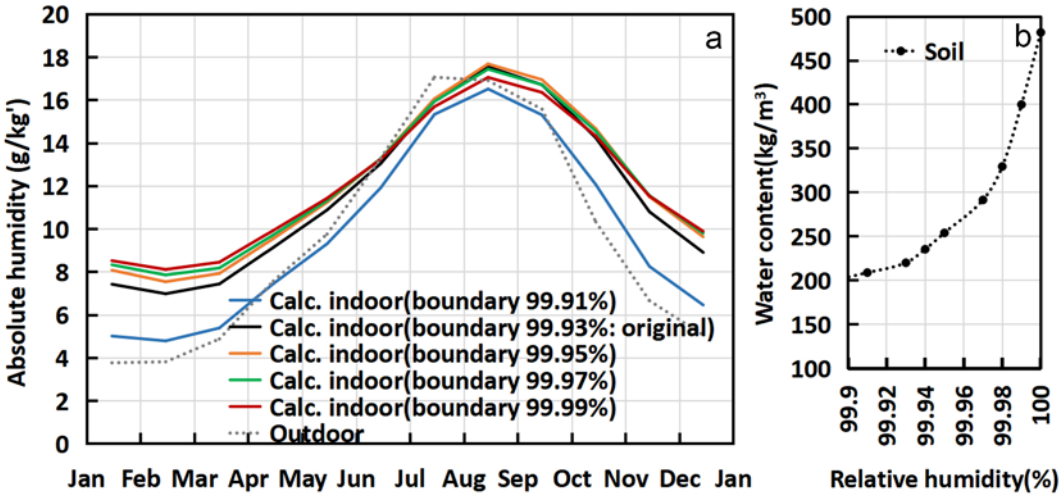

Figure 12. (a) Calculated monthly average indoor absolute humidity (sensitivity analysis of the ground boundary relative humidity); (b) Equilibrium moisture content of soil in the model [32].

4.1.2 Influence of ventilation on the indoor temperature and absolute humidity

In our target room, the windows and doors were closed to the outdoor air, and there was no mechanical ventilation. Therefore, the air exchange rate with the outdoor air was low throughout the year. A sensitivity analysis of the ventilation rate was performed, as shown in Figure 13, and the ventilation rate was sensitive to the indoor absolute humidity but not to the indoor air temperature (data plot not shown). Thus, the relative humidity changed with the absolute humidity. In the original case, the ventilation rate was set at 0.15 ACH, and the calculated results best agreed with the measured results.

With a ventilation rate of 0.5 ACH the indoor absolute humidity in winter was reduced to a level similar to the outdoor absolute humidity, and the indoor absolute humidity in summer was slightly higher than in the original case (0.15 ACH). When the ventilation rate increased from 0.5 ACH to 1 ACH, the indoor absolute humidity did not change significantly.

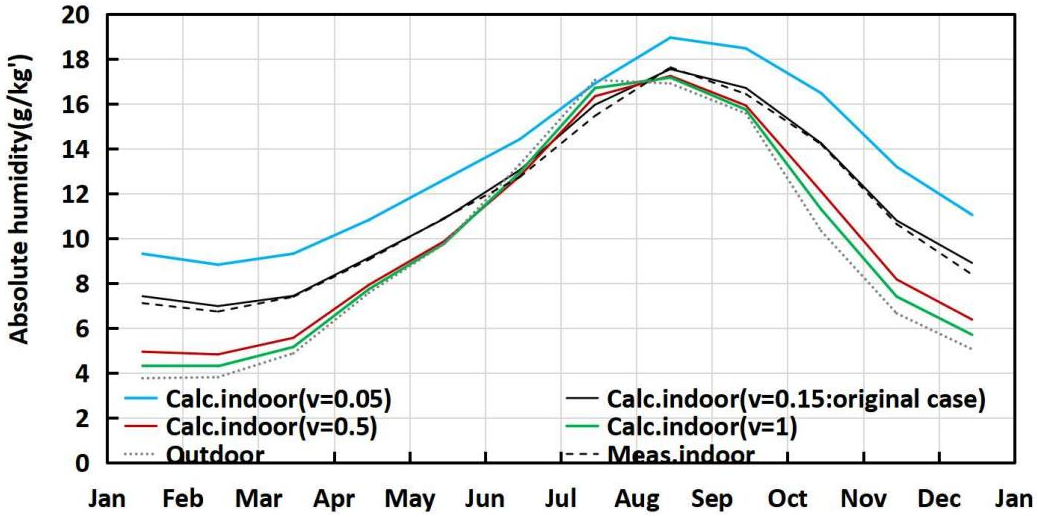

Figure 13. Calculated monthly average indoor absolute humidity (sensitivity analysis of the ventilation rate) (2016).

4.1.3 Influence of the area proportion between the walls in contact with the ground and the walls facing the outdoor air

The calculated results show that the heat and moisture fluxes from the envelopes in contact with the ground and those not in contact with the ground have different effects on the indoor temperature and humidity. In particular, the contribution of the

moisture flux from envelopes in contact with the ground to the indoor moisture balance was relatively large, and the heat flux from the wall facing the outdoor air significantly affected the indoor temperature. Additional analyses were performed to investigate the influence of different types of envelopes on the indoor climate. The area of the wall in contact with the outdoor air and that of the walls in contact with the ground were determined differently than in the original case. When the room volume was kept constant, the interior envelopes, representing 39 % of the envelope area, were replaced either by walls in contact with the ground or by walls in contact with the outdoor air.

As shown in Figure 14, the calculation case in which the area proportion of the walls in contact with the ground was increased compared to the original case showed that the heat capacity of the ground increased the indoor relative humidity throughout the year, whereas in winter, the moisture flux increased, and in summer the room temperature decreased.

Furthermore, the calculation case in which the area proportion of the walls facing the outdoor air was compared to the original case showed that the relative humidity became lower throughout the year than in the original case because of the lower influence of the ground. Thus, the problems with high humidity in underground spaces could have different causes depending on the season.

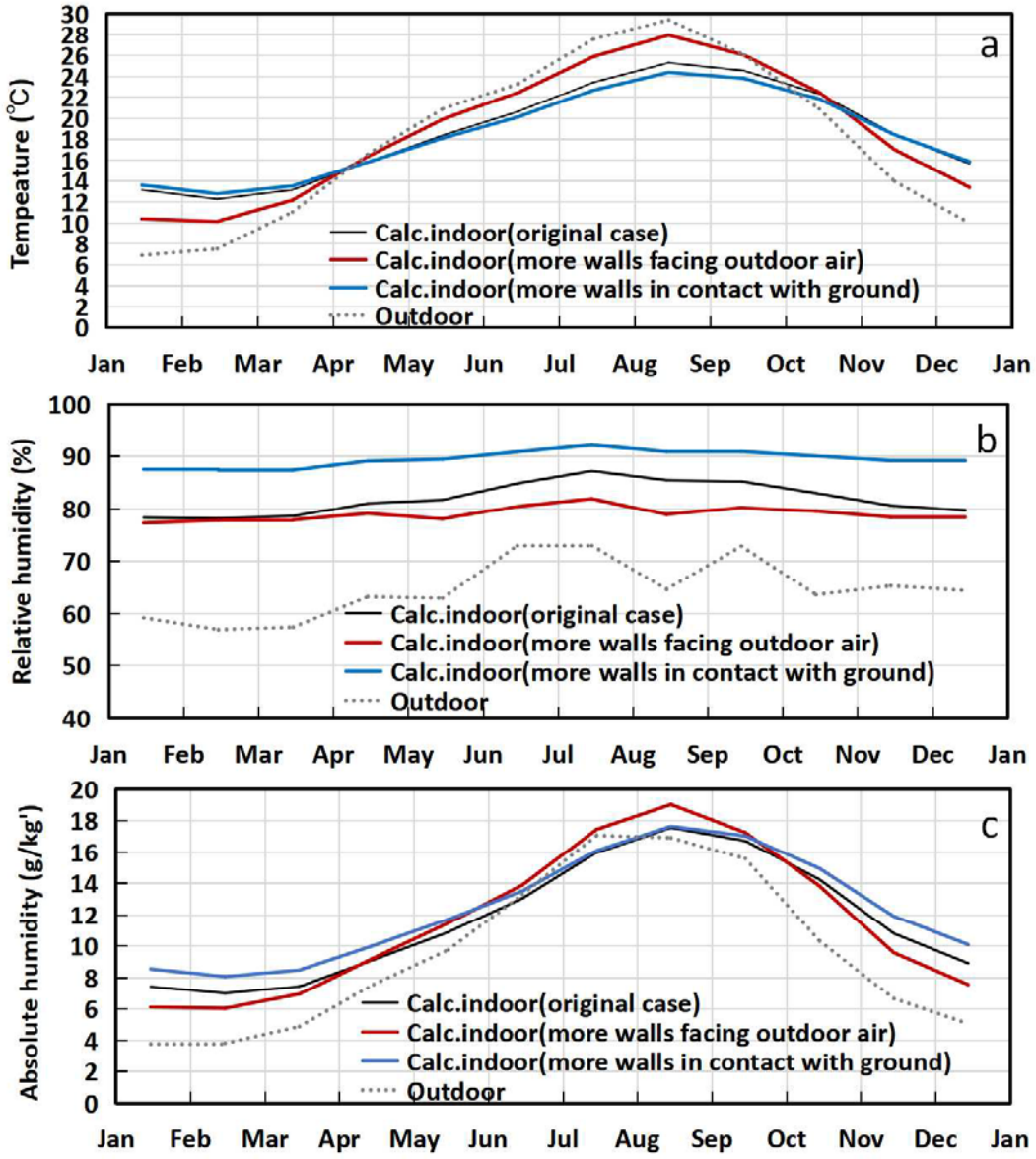

Figure 14. Calculated monthly average indoor (a) temperature, (b) relative humidity, and (c) absolute humidity (sensitivity analysis of the area of the walls in contact with the ground and that in contact with the outdoor air) (2016).

4.2 Limitations and representativeness of this study

Owing to the limitation of the computational load in this study, the indoor hygrothermal environment of the room was analyzed by applying the one-dimensional coupled heat and moisture transfer calculation to the ground and envelopes of the semi-underground room, considering the influence of heat and moisture transfer between the ground and envelopes of the room. This one-dimensional calculation neglected the influence of the hygrothermal capacity of the ground around the corners and edges of the room, as well as the three-dimensional properties of the heat and moisture flux in the materials of the envelope around the corners and edges of the room, possibly leading to an underestimation of the total heat and moisture transfer between the ground and room. In the future, influences such as local condensation at the corners or edges of the envelopes in contact with the ground should be determined by three-dimensional calculations.

In this study, the hygrothermal analysis was applied for uninhabited conditions without considering the additional influence of inhabitants' activities to clarify the characteristics and mechanism of moisture transfer from the ground. In inhabited conditions, moisture generation from inhabitants increases the indoor humidity, and the increase in indoor heat generation, larger ventilation rate, and the influence of cooling (dehumidification) will modify the indoor humidity. The results could vary from inhabited cases. In this paper, the fundamental behavior of moisture flux from the wall in contact with the ground was studied in a simple condition without inhabitants. In the future, calculations of other cases considering the additional influence factors owing to the inhabitants will be conducted based on the findings of this study.

4.3 Suggestions for improving the moisture environment of underground spaces suffering from excessive humidity

As a basic countermeasure to prevent moisture damage in semi-underground spaces, an insulating layer is usually installed inside the wall in contact with the ground, as is the case with our target room. This is effective for summer. However, it is inadequate for winter because the effects of moisture flux from the ground on indoor humidity in underground spaces are significant, as this study shows.

The results of this study suggest that masking the moisture transfer (both liquid and vapor) from the ground by adding a moisture-proof layer inside the envelope in contact with the ground could be a measure to improve the moisture environment in underground spaces, especially in winter. However, the secondary risk that could arise after the installation of such a moisture-proof layer should be considered.

5. Conclusion

To quantify the effects of moisture transfer from the ground on indoor humidity and hygrothermal behavior of the building envelopes, indoor temperature and humidity were measured for an unoccupied, semi-underground apartment in several rooms of the apartment over four years. In addition, by developing a hygrothermal model for a system that included both the semi-underground room and the surrounding ground, the moisture flux from the ground was evaluated, and the mechanism of the moisture balance of the underground space was clarified. The results of this study can be summarized as follows:

- The measured annual average of indoor absolute humidity was higher than that of the outdoor air, indicating that the ground acted as a moisture source for the indoor space, resulting in high humidity in the rooms in contact with the ground, despite no moisture being generated by human activities.
- The hygrothermal model of the target room and the surrounding ground was validated by comparison with the measured data, and the calculations based on the model revealed that the influence of the moisture flux originating from the ground on the indoor humidity of the target semi-underground room was noticeable. Based on the calculated moisture balance of the target room, the moisture generated from the envelopes in contact with the ground was highest from autumn to spring and contributed significantly to the high indoor humidity, especially in winter. Furthermore, it reached 19 g/(m^2 · day) and accounted for more

than 80 % of the total indoor moisture gain for an unoccupied case with a minimal ventilation rate and no moisture generation from human activities. The noticeable moisture flow from the ground was strong enough to cause severe condensation on the window surface and excessive humidity to the envelopes facing the outdoor air during the winter, despite no additional indoor moisture sources owing to occupant activity.

- The moisture buffering effect of the interior envelopes contributed to lower indoor relative humidity in summer, but their influence on the moisture balance of the underground space in winter was at most 18 %.
- The heat capacity of the ground contributed to higher indoor relative humidity throughout the year. In winter, the moisture flux from the wall in contact with the ground increased owing to the high temperature of the ground, whereas in summer, the lower indoor air temperature owing to heat capacity of the ground caused high relative humidity.

The novelty of this study is on the quantification of the moisture flux from the ground in a real uninhabited underground room and the clarification of the mechanism of its seasonal characteristics based on the calculation results of a model validated by the measured indoor temperature and humidity over a year. In conclusion, the influence of moisture from the ground is significant and should not be neglected when analyzing the mechanism of moisture-related problems in unoccupied underground space or proposing appropriate countermeasures. Furthermore, indoor humidity can be effectively reduced by eliminating moisture transfer from the ground, though the risks associated with creating a moisture-proof layer should be clearly elaborated in future studies.

References

[1] R. Kumar, S. Sachdeva, and S. C. Kaushik, "Dynamic earth-contact building: A sustainable low-energy technology," Building and Environment, vol. 42, no. 6, pp. 2450-2460, 2007.

[2] C. van Dronkelaar, D. Cóstola, R. A. Mangkuto, and J. L. M. Hensen, "Heating and cooling energy demand in underground buildings: Potential for saving in various climates and functions," Energy and Buildings, vol. 71, pp. 129-136, 2014.

[3] A. Benardos, I. Athanasiadis, and N. Katsoulakos, "Modern earth sheltered constructions: A paradigm of green engineering," Tunnelling and Underground Space Technology, vol. 41, pp. 46–52, 2014.

[4] J. Yu, Y. Kang, and Z. Zhai, "Advances in research for underground buildings: Energy, thermal comfort and indoor air quality," Energy and Buildings, vol. 215, p.109916, 2020.

[5] J. Zhu, L. Tong, R. Li, J. Yang, and H. Li, "Annual thermal performance analysis of underground cave dwellings based on climate responsive design," Renewable Energy, vol. 145, pp. 1633-1646, 2020.

[6] D. V. L. Hunt, L. O. Makana, I. Jefferson, and C. D. F. Rogers, "Liveable cities and urban underground space," Tunnelling and Underground Space Technology, vol. 55, pp. 8-20, 2016.

[7] S. Yu, Z. Yu, P. Liu, and G. Feng, "Influence of environmental factors on wall mould in underground buildings in Shenyang City, China," Sustainable Cities and Society, vol. 46, p.101452, 2019.

[8] Y. Li, D. Ogura, S. Hokoi, J. Wang, and T. Ishizaki, "Predicting hygrothermal behavior of an underground stone chamber with 3-D modeling to restrain water-related damage to mural paintings," Journal of Asian Architecture and Building Engineering, vol. 13, no. 2, pp. 499-506, 2014.

[9] Petri J. Annila, Jukka Lahdensivu, Jommi Suonketo, Matti Pentti, Juha Vinha, "Need to repair moisture- and mould damage in different structures in finnish public buildings," Journal of Building Engineering, vol.16, pp 72-78, 2018.

[10] H. Zhang, J. Liu, C. Li, and Z. Lian, "Long-term investigation of moisture environment in underground civil air defence work," Indoor and Built Environment, vol. 26, no. 6, pp. 744-757, 2017.

[11] M. H. Adjali, M. Davies, S. W. Rees, and J. Littler, "Temperatures in and under a slab-on-ground floor: two- and three-dimensional numerical simulations and comparison with experimental data," Building and Environment, vol. 35, no. 7, pp. 655-662, 2000.

[12] W. P. Bahnfleth, "Three-dimensional modelling of heat transfer from slab floors," Ph.D. Dissertation, Dept. Mechanical Science and Engineering, University of Illinois Urbana-Champaign, Urbana, United States, 1989.

[13] S. W. Rees, Z. Zhou, and H. R. Thomas, "Ground heat transfer: A numerical simulation of a full-scale experiment," Building and Environment, vol. 42, no. 3, pp. 1478-1488, 2007.

[14] S. Andolsun, C. H. Culp, J. S. Haberl, and M. J. Witte, "EnergyPlus vs DOE-2.1e: The effect of ground coupling on cooling/heating energy requirements of slab-on-grade code houses in four climates of the US," Energy and Buildings, vol. 52, pp. 189-206, 2012.

[15] A. Al-Anzi and M. Krarti, "Local/global analysis of transient heat transfer from building foundations," Building and Environment, vol. 39, no. 5, pp. 495-504, 2004.

[16] Y. Yuan, H. Ji, Y. Du, and B. Cheng, "Semi-analytical solution for steady-periodic heat transfer of attached underground engineering envelope," Building and Environment, vol. 43, no. 6, pp. 1147-1152, 2008.

[17] D. Chen, "Dynamic three-dimensional heat transfer calculation for uninsulated slab-on-ground constructions," Energy and Buildings, vol. 60, pp. 420-428, 2013.

[18] ASHRAE handbook—fundamental (SI edition), American Society of Heating, Refrigerating and Air-Conditioning Engineers Inc., Atlanta, 18.35-18.40, 2017.

[19] EN ISO 13370, Thermal performance of buildings-heat transfer via ground - Calculation methods, 2017.

[20] S. W. Rees, Z. Zhou, and H. R. Thomas, "The influence of soil moisture content variations on heat losses from earth-contact structures: an initial assessment," Building and Environment, vol. 36, no. 2, pp. 157-165, 2001.

[21] Jia Yu, Yanming Kang, Zhiqiang (John) Zhai, "Comparison of ground coupled heat transfer models for predicting underground building energy consumption," Journal of Building Engineering, vol. 32, 2020.

[22] G. H. dos Santos and N. Mendes, "Simultaneous heat and moisture transfer in soils combined with building simulation," Energy and Buildings, vol. 38, no. 4, pp. 303-314, 2006.

[23] H. Janssen, J. Carmeliet, and H. Hens, "The influence of soil moisture in the unsaturated zone on the heat loss from buildings via the ground," Journal of Thermal Envelope and Building Science, vol. 25, no. 4, pp. 275-298, 2002.

[24] H. Janssen, J. Carmeliet, and H. Hens, "The influence of soil moisture transfer on building heat loss via the ground," Building and Environment, vol. 39, no. 7, pp. 825-836, 2004.

[25] L. S. Shen and J. W. Ramsey, "An investigation of transient, two-dimensional coupled heat and moisture flow in the soil surrounding a basement wall," International Journal of Heat and Mass Transfer, vol. 31, no. 7, pp. 1517-1527, 1988.

[26] L. Shi et al., "Analysis of moisture buffering effect of straw-based board in civil defence shelters by field measurements and numerical simulations," Building and Environment, vol. 143, pp. 366-377, 2018.

[27] D. Ogura, T. Terashima, M. Mizuhata, and M. Matsumoto, "Field experiment of heat and moisture behavior of the underground space and its surrounding ground," Journal of Architecture and Planning (Transactions of AIJ), vol. 65, pp. 35-41, 2000.

[28] D. Ogura and M. Matsumoto, "An analysis of heat and moisture behavior of underground space: effects of moisture damper arrangement and depth of water table," Journal of Architecture and Planning (Transactions of AIJ), vol. 529, pp. 23-29, 2000. (in Japanese, with English abstract)

[29] D. Ogura, S. Mino, T. Matsushita, M. Mizuhata, and M. Matsumoto, "Analysis of heat and moisture behavior in the underground space and its surrounding ground," Journal of Architecture and Planning (Transactions of AIJ), vol. 66, pp. 15-21, 2001. (in Japanese, with English abstract)

[30] F. Fedorik, R. Heiskanen, A. Laukkarinen, and J. Vinha, "Impacts of multiple refurbishment strategies on hygrothermal behaviour of basement walls," Journal of Building Engineering, vol. 26, p.100902, 2019.

[31] H. L. Zhang, W. M. Marci, and X. Z. Fu, "Modeling of the hygrothermal absorption and desorption for underground building envelopes," Energy and Buildings, vol. 42, no. 8, pp. 1215-1219, 2010.

[32] Fraunhofer. WUFI PLUS. https://wufi.de/en/ (Accessed in April 2019)

[33] H.M. Künzel, "Simultaneous heat and moisture transport in building components one- and two-dimensional calculation using simple parameters, " Fraunhofer IRB Verlag, Stuttgart, 1995.

[34] M. K. Kumaran, IEA ANNEX 24 Energy conservation in building and community systems, Final report, vol. 3 Task 3: Material properties, 2001.

[35] M. Matsumoto and A. Iwamae, "An analysis of temperature and moisture variations in the ground under natural climatic conditions," Energy and Buildings, vol. 11, no. 1, pp. 221-237, 1988.

[36] Shanshan Shi, Chen Chen, and Bin Zhao, "Air infiltration rate distributions of residences in Beijing, Building and Environment," vol. 92, pp, 528-537, 2015.